

Chemical composition of evolved stars of high galactic latitude^{*}

Sunetra Giridhar¹ and A. Arellano Ferro²

¹ Indian Institute of Astrophysics, Bangalore 560034, India
e-mail: giridhar@iiap.ernet.in

² Instituto de Astronomía, Universidad Nacional Autónoma de México, Apdo. Postal 70-264, D.F. CP 04510, México
e-mail: armando@astroscu.unam.mx

Received 19 June 2004 / Accepted 11 July 2005

ABSTRACT

We have carried out abundance analysis for a sample of high galactic latitude supergiants in search of evolved stars. We find that HD 27381 has atmospheric parameters and an abundance pattern very similar to that of the post-AGB star HD 107369. HD 10285 and HD 25291 are moderately metal-poor and show the influence of mixing that has brought the products of NeNa cycle to the surface. The high galactic latitude B supergiant HD 137569 shows selective depletion of refractory elements normally seen in post-AGB stars. We find that the high velocity B type star HD 172324 shows moderate deficiency of Fe group elements but the CNO abundances are very similar to that of disk B supergiants. The observed variations in the radial velocities, transient appearance of emission components in hydrogen line profiles and doubling of O I lines at 7774 Å support the possibility of this star being a pulsating variable or a binary star.

Key words. stars: AGB and post-AGB – stars: chemically peculiar – stars: abundances – stars: individual HD 10132, HD 10285, HD 12533, HD 25291, HD 27381, HD 137569, HD 159251, HD 172324

1. Introduction

There has been considerable interest in the chemical composition studies of stars in various stages of evolution, as they provide diagnostic tools to examine the predictions made by theories of stellar evolution. Of particular interest among evolved stars are the post-AGB stars, where the abundance peculiarities resulting from evolutionary processes manifest on a relatively short time scale. A fairly large number of post-AGB stars have been studied in the last two decades. Within them, a few distinct subgroups have been identified. One group containing stars with $C/O > 1$ displays considerable enhancement of s-process elements. Typical examples are HD 56126, HD 187785 and IRAS 06530-0213 (see Reddy et al. 2002; and Van Winckel 2003 for an overview). These objects show two peaks in their Spectral Energy Distribution (SED) and their metallicity ranges between $[Fe/H] = -0.3$ and -1.0 . The O-rich post-AGB stars ($C/O < 1$) do not display s-process enhancement but display a double humped SED and metallicity range similar to that seen in C-rich AGB stars. The typical examples are 89 Her, HD 161796, HD 133656, SAO 239853 etc. Yet another group of post-AGB stars with $C/O \sim 1$ show abundance peculiarities caused by selective removal of condensable elements e.g. BD+39° 4926, HR 4049, HD 44179, HD 46703, HD 52961 (references to the individual objects can be found in a review paper by Van Winckel 2003). Although a large fraction of them

are known to be binaries and the presence of IR fluxes lend further support to the idea of circumbinary disk as the site of dust-gas separation, lack of detected IR for BD+39°4926 is difficult to explain via a binary hypothesis. Many RV Tau stars like AD Aql, AC Her, EP Lyr, AR Pup, UY CMa, HP Lyr, DY Ori, BZ Sct, RU Cen and SX Cen (see Giridhar et al. 1998, 2000, 2005; Maas et al. 2002, and references therein) also show very similar abundance patterns. Although AC Her, V Vul, RU Cen and SX Cen are RV Tauri stars with a detected binary companion, the frequency of binaries in RV Tauri stars is yet to be determined.

A fourth group contains hot post-AGB stars which are metal-poor with remarkably high carbon deficiency (McCausland et al. 1992; Conlon et al. 1991; Moehler & Heber 1998; Mooney et al. 2002). These stars also show considerable deficiency of N, O, Mg and Si although these deficiencies are not as large as seen for carbon. Examples of this group are PG 1323-086, LS IV -4°01 and LB 3139. These objects are believed to be evolving on low mass post-AGB evolutionary tracks.

Within post-AGB stars, those evolving from relatively massive main sequence stars ($\sim 7 M_{\odot}$) would have a shorter transition time before becoming planetary nebula (PNe) and would be surrounded by dense circumstellar shells. The very stringent criteria of low gravity, high galactic latitude, strong IR excess and photometric variabilities given in Trams et al. (1991) and their location in the IRAS two color diagram of van der Veen & Habing (1988) has been extremely useful in detecting the new

^{*} Based on observations obtained at the Haute-Provence Observatory, France.

Table 1. Basic data for the sample stars.

Star	Sp.T.	V (mag)	l ($^{\circ}$)	b ($^{\circ}$)	IRAS	$12\ \mu$ (Jy)	$25\ \mu$ (Jy)	$60\ \mu$ (Jy)	$100\ \mu$ (Jy)
HD 10132	G5	7.75	132.57	-20.3	02008+4205	.69	.39	.40	1.00
HD 10285	A5	8.60	128.59	+1.12					
HD 12533	K3IIIb	2.26	136.96	-18.56	01285+6115	98.55	23.96	3.59	1.16
HD 25291	F0II	5.04	145.51	+5.03	04002+5901	1.60	.41	0.40L	2.09L
HD 27381	F2	7.55	161.64	-8.07	04175+3827	.81	.32L	.40L	2.19L
HD 137569	B5III:	7.91	21.87	+51.93					
HD 159251	G5	7.24	117.33	+29.32	17193+8439	.52	.16	.40L	3.78L
HD 172324	B9Ib	8.16	66.18	+18.58					

C and O-rich post-AGB stars described above. However, there are interesting stars like BD+39 $^{\circ}$ 4926 with no IR detection and other hot post-AGB stars that do not exhibit large IR excess. It is likely that these stars have evolved from the low-mass end of post-AGB domain (1.5 to 3 M_{\odot}). These stars would have longer transition times and would have lost most of their circumstellar envelope before moving towards the PNe region. With a longer transition period, their detection probability would be higher.

Our sample, therefore, contains high galactic latitude, low gravity stars without insistence on excess IR. Although HD 10132, HD 25291 and HD 27381 do have larger than stellar fluxes at $100\ \mu$ wavelengths, in most cases the excess IR is smaller than the measurement errors. Similarly for HD 12533 and HD 159251 the observed SED indicates that the observed IR fluxes do not translate into IR excess larger than the measurement errors. A few high velocity and high galactic latitude supergiants like HD 10285, HD 137569 and HD 172324 without IR detection are also included but these are known to show light variabilities. In a previous paper (Arellano Ferro et al. 2001; Paper I) we have presented our detailed abundance analysis for the interesting post-AGB stars HD 158616 and HD 172481. In the same paper, we had reported metal and carbon deficiency for HD 172324 and suggested that a more comprehensive analysis was required. With extended spectral coverage we have now made a more complete analysis of this object.

The present paper is organized as follows: in Sect. 2 the observations and reduction techniques are briefly described and a discussion of photometric estimates of the initial values of the effective temperature and the uncertainties in the derived abundances is given. Section 3 contains the detailed discussion on the elemental abundances of each object in the sample. Section 4 summarizes our findings and derived conclusions.

2. Observations and data reduction

Table 1 contains the list of stars studied in this work, their spectral types, magnitudes, galactic positions and, if available, the IRAS infrared fluxes.

The observational material for this work was obtained during October 5–October 10, 2000 with the 1.93 m telescope of the Haute-Provence Observatory (OHP), which is equipped with the high resolution (42 000) echelle spectrograph

Table 2. Derived physical parameters for program stars.

Star	T_{eff} (K)	$\log g$	ξ (km s^{-1})	$V_r(\text{hel})$ (km s^{-1})	$V(\text{LSR})$ (km s^{-1})
HD 10285	7750	1.5	3.5	-69.9	-64.2
HD 25291	7250	1.5	3.5	-19.2	-18.3
HD 27381	7500	1.0	4.0	-5.4	-11.4
HD 137569	12 500	3.0	8.0	-45.7	-30.2
HD 137569 †	12 000	3.0	7.0	-55.2	-39.6
HD 172324*	11 000	2.5	5.0	-126.1	-106.4
	11 500	2.5	7.5	-117.3	-97.5
	10 500	2.5	5.4	-139.0	-119.3
	10 500	2.5	6.8	-105.2	-85.7
				-152.1	-132.5 $^+$
HD 10132	5000	2.0	1.0	-70.2	-64.5
HD 12533	4250	2.0	1.8	-11.2	-10.9
HD 159251	4800	2.75	1.2	-39.2	-27.6

† – From McDonald spectrum obtained in 2004. * – Four independent analyses carried out for different epochs are included. The first two are from Paper I. The second two are from the present work. + Radial velocity measured on a 17 000 resolution spectrum obtained at San Pedro Mártir Observatory on November 18, 2000.

ELODIE. Details about the performance and characteristics of the instrument have been thoroughly described by Baranne et al. (1996). These spectra were reduced using spectroscopic data reduction tasks available in the IRAF package. At our request, additional spectra of HD 172324 and HD 137569 were obtained by Dr. E. Reddy and Dr David Yong using the 2d Coudé echelle spectrograph of 2.7 m telescope at McDonald observatory described in Tull et al. (1995). These spectra have resolution of 60 000.

2.1. Spectroscopic reductions

For details about the reductions of our spectra, from the raw CCD images to the measurement of equivalent widths and a discussion of their uncertainties, the reader is referred to Paper I.

2.2. Determination of atmospheric parameters

As is well-known, the line strengths are affected by atmospheric parameters like the effective temperature (T_{eff}), gravity ($\log g$) and microturbulent velocity (ξ). It is therefore necessary to determine these parameters before using line strengths for abundance determinations.

The present sample contains stars with a large range in temperatures. The criteria used for determining the atmospheric parameters for hot members ($T_{\text{eff}} > 10\,000$ K) were different from those at the cooler side. For stars cooler than 8000 K the Fe-group elements like Ti, Cr and Fe have a large number of lines covering a range in line strengths, excitation potential and two stages of ionization. We have therefore followed the standard procedure of estimating ξ by requiring that the derived abundances are independent of line strengths. The temperature and gravity were estimated by eliminating the dependence of computed abundances on lower excitation potentials and requiring that the neutral and ionized lines give the same abundances.

Starting values of T_{eff} and $\log g$ are obtained from the photometric indices. For stars of intermediate temperatures, we possess unpublished empirical calibrations of reddening-free Strömgren photometric indices [m_1], [c_1] and H_β , in terms of T_{eff} . These calibrations were calculated for 41 stars with spectral types between A0 and K0 and luminosity classes I or II. The effective temperatures of calibrating stars were determined from 13-color photometry (Bravo-Alfaro et al. 1997).

For hotter members we used line strengths and profiles of hydrogen and helium lines and the ionization equilibrium of Si I/Si II, Mg I/Mg II whenever the related spectral data were available.

We have used the 2002 version of the spectrum synthesis code MOOG written by Sneden (1973) in both line and spectrum synthesis mode for stars cooler than 8000 K. We used LTE model atmospheres of Kurucz (1993), and the revised list of oscillator strengths of Luck (2002) for Fe-group elements. For lighter elements we used $\log gf$ values compiled by Wiese et al. (1996). For Fe I lines we preferred $\log gf$ values given in Lambert et al. (1996) or Luck (2002) for Fe II we used the data of Giridhar & Arellano Ferro (1995) and those in Table A2 of Lambert et al. (1996). For heavier elements we used the ValD-2 database (Kupka et al. 1999) in addition to Luck (2002).

2.3. Uncertainties in the elemental abundances

For most of the spectra employed in the abundance analysis the S/N ratio is in the 50–100 range. For the stars with $4500 \text{ K} < T_{\text{eff}} < 8000 \text{ K}$ we could find clean unblended lines for a large number of elements and we believe that the measured equivalent widths have an accuracy of 5–8%. The sensitivity of derived abundances to changes in the model atmosphere parameters are described in Table 3 using a small set of lines with well determined atomic data. The last column of Table 3 shows the errors corresponding to an 8% error in equivalent width measurements. It is representative of the basic precision that can be attained with the instrumental setup. We find that at T_{eff} of 5000 K, a change in temperature of 250 K causes

the change in line strength which is larger than the measurement errors of line strengths. These changes have been presented as changes in abundances caused by ΔT_{eff} in Col. 6 of Table 3. Similarly, Cols. 7 and 8 are indicative of sensitivities of line strengths to changes in $\log g$ by 0.5 and ξ by 0.5 km s^{-1} . The spectra of HD 10132, HD 12533 and HD 159251 had clean unblended lines for all representative atoms covering a good range in equivalent widths, excitation potential and two stages of ionizations for many elements (Sc, Ti, V, Cr, Fe). Hence for these three stars the atmospheric parameters can be measured with accuracies indicated in Table 3.

HD 25291, HD 10285 and HD 27381 have temperatures in 7000 K to 7500 K range. For these stars, the spectra are much cleaner, but not as scanty as to prevent us from getting the required range in line strengths, excitation potentials and two stages of ionisation. We have used neutral and ionised lines of Mg, Si, Cr and Fe to derive the gravities. For these stars the temperatures are not large enough for the lines to develop strong wings making line strengths inaccurate. At the temperature of 7500 K, we find that the line strengths change by a larger amount if the temperature is changed by 250 K. These changes (presented as changes in abundances) are much larger than the measurement errors of the line strengths and therefore are easily discernible. We are limited by the coarseness of the grid of model atmospheres. A change of $\log g$ by 0.5 causes changes in line strengths that are twice the error of line strength measurements and hence is easily discernible. We have used additional temperature and gravity constraints such as the strengths and profiles of H_γ and H_δ to further improve the accuracy of these parameters. We have shown in Fig. 1 the loci of temperatures and gravities derived using different criteria. The adopted value of temperature and gravity is indicated by the asterisk. The gravities are estimated with an accuracy of ± 0.25 dex through profile fitting of H_γ and H_δ lines. At 7500 K, as one can see from Table 3, the calculated abundances are less sensitive to the changes in microturbulent velocities and hence our estimate of ξ may have an uncertainty of $1\text{--}2 \text{ km s}^{-1}$.

The errors in gf values vary from element to element. For Fe I lines, experimental values of accuracies better than 5% do exist, for other Fe-peak elements the range in errors could be within 10 to 20%. For heavier elements, particularly for s -process elements, the errors could be larger than 25%. Hence for Fe-peak elements with a large number of lines measured and good gf estimates available, abundances can be estimated with an accuracy of 0.15 to 0.2 dex. For the elements where fewer lines are available, like s -process elements, the uncertainty could be ± 0.3 dex or more.

We therefore believe that our abundance estimates for stars HD 10132, HD 12533, HD 159251, HD 10285, HD 25291 and HD 27381 have accuracies within 0.2 and 0.4 dex depending upon the number of lines measured and the quality of the gf values available.

For stars hotter than 10000 K the lines are fewer and have shallower profiles with extended wings. Hence the line strengths cannot be measured as accurately. We have therefore estimated the errors in the calculated abundances caused by the errors of equivalent measurements using 16% as the typical accuracy of line strength measurements. Since the spectrum

Table 3. Sensitivity of the calculated abundances to the changes in the atmospheric parameters.

HD 10132		Adopted	parameters		$T_{\text{eff}} = 5000 \text{ K}$	$\log g = 2.5$	$\xi = 1.0 \text{ km s}^{-1}$	
Wavelength	Species	EP	$W_{\lambda} \text{ m\AA}$	$\log \epsilon$	$\Delta T_{\text{eff}} + 250 \text{ K}$	$\Delta \log g + 0.5$	$\Delta \xi + 0.5$	$\Delta W_{\lambda} + 8\%$
5867.57	CaI	2.93	43.2	6.55	+0.20	-0.20	-0.06	+0.08
6169.04	CaI	2.52	116.5	6.48	+0.27	-0.27	-0.19	+0.13
5441.32	FeI	4.31	52.0	7.47	+0.22	-0.19	-0.12	+0.10
6054.07	FeI	4.37	24.0	7.58	+0.19	-0.18	-0.04	+0.05
4631.48	FeI	4.37	35.3	7.64	+0.19	-0.19	-0.07	+0.06
5294.56	FeI	3.64	32.2	7.56	+0.23	-0.23	-0.06	+0.06
5320.03	FeI	3.64	42.0	7.46	+0.24	-0.23	-0.09	+0.07
6411.66	FeI	3.65	152.0	7.46	+0.30	-0.28	-0.17	+0.10
6084.12	FeII	3.20	42.3	7.41	-0.08	+0.14	-0.11	+0.07
6149.25	FeII	3.89	52.6	7.38	-0.11	+0.18	-0.16	+0.10
6204.64	NiI	4.09	39.6	6.17	+0.19	-0.14	-0.08	+0.07
6175.42	NiI	4.09	66.0	6.18	+0.22	-0.16	-0.19	+0.12
HD 27381		Adopted	parameters		$T_{\text{eff}} = 7500 \text{ K}$	$\log g = 1.0$	$\xi = 4.0 \text{ km s}^{-1}$	
Wavelength	Species	EP	$W_{\lambda} \text{ m\AA}$	$\log \epsilon$	$\Delta T_{\text{eff}} + 250 \text{ K}$	$\Delta \log g + 0.5$	$\Delta \xi + 0.5$	$\Delta W_{\lambda} + 8\%$
6122.23	CaI	1.89	40.2	5.81	+0.44	-0.20	-0.01	+0.04
6162.18	CaI	1.90	56.2	5.78	+0.45	-0.21	-0.02	+0.04
6462.57	CaI	2.52	44.2	5.78	+0.43	-0.21	-0.02	+0.05
5328.04	FeI	0.93	140.2	6.88	+0.40	-0.14	-0.09	+0.12
5569.62	FeI	3.42	34.0	6.80	+0.30	-0.15	-0.01	+0.04
5572.84	FeI	3.40	55.0	6.84	+0.34	-0.15	-0.01	+0.05
5162.27	FeI	4.18	44.0	6.96	+0.32	-0.15	-0.01	+0.05
5415.27	FeI	4.39	63.0	6.91	+0.32	-0.15	-0.02	+0.05
4620.51	FeII	2.83	127.0	6.82	+0.16	+0.08	-0.08	+0.09
4632.68	FeII	2.89	94.0	6.89	+0.17	+0.07	-0.04	+0.06
6419.25	FeII	3.89	105.0	6.89	+0.15	+0.08	-0.04	+0.10
HD 137569		Adopted	parameters		$T_{\text{eff}} = 12000 \text{ K}$	$\log g = 2.5$	$\xi = 7.0 \text{ km s}^{-1}$	
Wavelength	Species	EP	$W_{\lambda} \text{ m\AA}$	$\log \epsilon$	$\Delta T_{\text{eff}} - 500 \text{ K}$	$\Delta \log g + 0.5$	$\Delta \xi + 1.0$	$\Delta W_{\lambda} + 16\%$
7423.64	NI	10.33	33.8	6.55	+0.15	+0.33	-0.01	+0.09
7442.29	NI	10.33	50.0	6.49	+0.16	+0.33	-0.02	+0.11
7468.31	NI	10.33	66.4	6.53	+0.16	+0.33	-0.02	+0.12
5330.74	O I	10.74	36.0	6.92	+0.14	+0.32	-0.02	+0.10
6155.99	O I	10.74	39.0	6.89	+0.16	+0.33	-0.02	+0.10
6156.78	O I	10.74	62.0	7.00	+0.15	+0.32	-0.03	+0.11
5014.03	SII	14.07	28.6	6.98	+0.11	+0.25	-0.01	+0.09
5432.80	SII	13.62	23.0	6.51	+0.13	+0.26	-0.03	+0.08
5606.11	SII	13.73	20.0	6.68	+0.13	+0.28	-0.03	+0.10
6578.05	CII	14.45	36.0	4.10	+0.34	+0.69	-0.04	+0.13
6582.88	CII	14.45	19.9	3.92	+0.34	+0.70	-0.02	+0.12

synthesis code MOOG was primarily written for late type stars and does not incorporate the opacities necessary for the flux computation of hot stars, we chose to use the SPECTRUM code which is described in Gray & Corbally (1994) for the analysis of hot stars HD 137569 and HD 172324. We were concerned about the systematic differences that might be caused by the use of these two different codes. We have therefore computed the spectrum of Vega using a stellar model with T_{eff} of 9400 K, $\log g$ of 3.9 and ξ of 2.0 km s^{-1} and the recent abundance estimates from the literature. The spectra computed using MOOG

and SPECTRUM codes were compared with the high resolution spectrum of Vega (Qiu et al. 1999a,b) in selected spectral regions containing important lines for many elements of interest. We found very satisfactory agreement for all elements with the the abundances derived using the two codes up to temperature of 8000 K. Hence we believe there is no systematic difference in estimated abundances caused by the use of two different codes. However at temperatures hotter than 10000 K the departure from LTE becomes important. We have applied the systematic corrections caused by the neglect of non-LTE and they

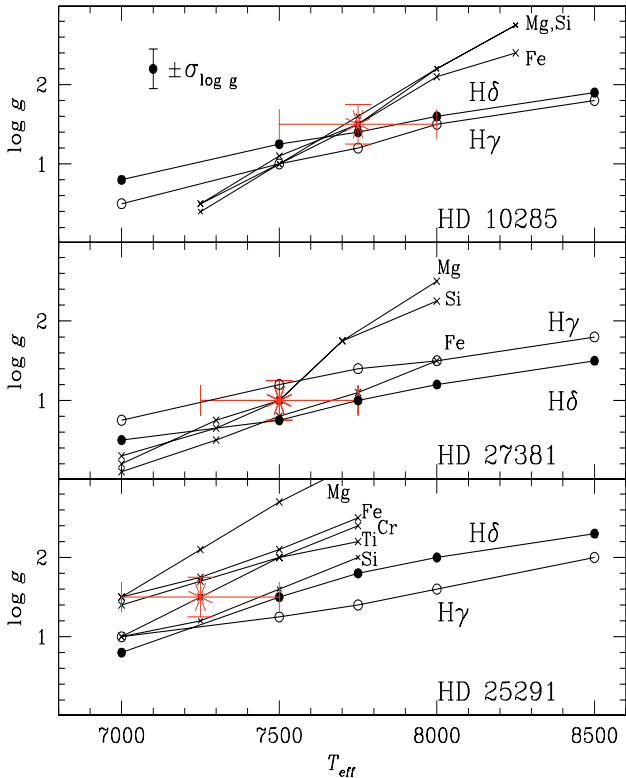


Fig. 1. Feature trends with variations in gravity and temperature. The asterisk indicates the adopted pair $T_{\text{eff}} - \log g$ for subsequent element abundance analysis. The Balmer line loci were obtained by fitting the observed lines with the Kurucz's (1993) models. The uncertainty in $\log g$ for a given temperature attained in this process is indicated by the error bar in the top panel.

are discussed in the subsection of each star. These effects and the relative paucity of lines of representative atoms results in larger measurement errors for the abundances for HD 172324 and HD 137569. Hence their estimated abundances may be accurate to only to one significant digit.

3. Derived elemental abundances

In this section, we present our abundance results for the individual stars. In the abundance Tables 4 and 6 the solar abundances were taken from the work of Grevesse et al. (1996) except for carbon and oxygen that were taken from Allende Prieto et al. (2002, 2001) respectively. The number of lines included in the calculations is represented by n .

3.1. HD 10285

HD 10285 is considered a high galactic latitude low-mass supergiant candidate by Bidelman (1990) based on its high Strömgen c_1 index (1.62). Our interest in this object has been aroused by its significantly large radial velocity (-58 km s^{-1}). As can be seen from Table 4 our analysis covers a large number of elements based on a large number of lines for many elements. Although the derived iron deficiency $[\text{Fe}/\text{H}] \sim -0.3$ is not very large, it is a high precision estimate. The star also shows noticeable relative enhancement of Na and S relative to

Fe. Non-LTE corrections for Na abundances at the temperature of 7750 K for the lines employed by us is ~ -0.16 as tabulated by Takeda & Takada-Hidai (1994). Hence the Na enhancement reported in Table 4 is not caused by the neglect of non-LTE effects but is a real effect. The enhancement of Na relative to Fe is possibly caused by the mixing of the NeNa-cycle products from the hydrogen burning region. We do not have evidence of evolution beyond the red giant stage for this star.

3.2. HD 25291

This star has been included in a number of investigations and the estimated temperatures lie in the 6700 K (Andrievsky et al. 2002) to 7600 K (Venn 1995a,b) range. Venn carried out a comprehensive abundance analysis covering many elements. Our analysis employs an even larger number of lines and extends to heavier elements. The carbon abundance derived by us is systematically smaller than the value derived by Venn (1995b) but the lines used by us are different. For silicon and oxygen we find good agreement with the values obtained by Venn. We find a relative enrichment of Na, Si and S, similar to that found in HD 10285. The abundance of s-process elements is essentially solar. We do not consider this object as a post-AGB star.

3.3. HD 27381

Although the SED generated using observed optical and IR color bands shows larger than stellar component fluxes at 12, 25 and 60μ , the error bars are too large to report IR excess. At 100μ the excess IR flux is larger than the measurement errors. We have derived carbon abundance by synthesizing the the $4765\text{--}4780 \text{ \AA}$ spectral region containing CI lines as shown in Fig. 2. Nitrogen abundances were derived using N I lines in the $7420\text{--}7470 \text{ \AA}$ region. As can be seen from the abundances presented in Table 4, this is a metal-poor star. Although $[\text{Fe}/\text{H}]$ of -0.7 is not very large, it is quite significant. Since the derived $[\text{Fe}/\text{H}]$ is very similar to the mean metallicity of thick disk population (Gilmore et al. 1995), we chose to compare elemental abundances for this star with those derived for thick disk stars by Prochaska et al. (2000). These authors give the mean $[\text{X}/\text{Fe}]$ for a large number of elements in their Table 19. Although HD 27381 shows enhancement of some α -elements like O, Si and S seen in the thick disk stars, it does not show relative enrichment of Mg and Ti. The observed $[\text{Si}/\text{Fe}]$ and $[\text{S}/\text{Fe}]$ are larger than their corresponding values in Prochaska et al.'s (2000) sample, and relative enhancement of Al is not seen, although $[\text{Ca}/\text{Fe}]$ agrees within the errors of the estimates. On the other hand, we find an indication of evolutionary effects in the form of enhanced N and Na abundances and carbon deficiency. A non-LTE correction of -0.4 is estimated by Venn (1995b) for the C I lines at the temperature of 7500 K, although this estimate was made for lines in 7100 \AA region. Hence the non-LTE $[\text{C}/\text{Fe}]$ would be even smaller than the $[\text{C}/\text{Fe}]$ of -0.4 given in Table 4. For N I lines used in the present work at 7500 K the non-LTE corrections are estimated as -0.3 indicating a non-LTE corrected $[\text{N}/\text{H}]$ of $+0.2$ and $[\text{N}/\text{Fe}]$ of $+0.9$. Hence we have a very distinct signature of CN processed material on the

Table 4. Elemental abundances of hotter stars.

Spe cies	log ϵ_{\odot}	HD 10285	HD 25291	HD 27381	HD 137569	HD 172324
		[X/H], <i>n</i> , [X/Fe]	[X/H], <i>n</i> , [X/Fe]	[X/H], <i>n</i> , [X/Fe]	[X/H], <i>n</i> , [X/Fe]	[X/H], <i>n</i> , [X/Fe]
C I	8.39	-0.27 ± 0.13, 3, +0.04	-0.71 ± 0.17, 5, -0.38	-1.04, <i>syn</i> , -0.37
C II	8.39	-0.2, <i>syn</i> , +2.8 :	-0.04, <i>syn</i> , +0.5
		-0.6*, <i>syn</i> , +2.4 :	-0.3*, <i>syn</i> , +0.2
N I	7.83	+0.50, <i>syn</i> , +1.20	+0.8 ± 0.06, <i>syn</i> , +3.8 :	+0.7 ± 0.16, <i>syn</i> , +1.2
		+0.2*, <i>syn</i> , +0.9	+0.2*, <i>syn</i> , +3.2 :	+0.1*, <i>syn</i> , +0.6
O I	8.69	-0.00 ± 0.03, 2, +0.30	-0.18 ± 0.01, 2, +0.15	-0.36 ± 0.03, 3, -0.3	+0.3 ± 0.16, 9, +3.3 :	+0.2 ± 0.07, 5, +0.8
					+0.1*, <i>syn</i> , +3.1 :	-0.1*, <i>syn</i> , +0.4
Ne I	8.09	+0.2 ± 0.14, 3, +3.2 :	+0.4 ± 0.16, 5, +0.9
Na I	6.33	+0.11 ± 0.04, 2, +0.41	+0.17 ± 0.05, 4, +0.50	-0.13 ± 0.04, 3, +0.54
Mg I	7.58	-0.19 ± 0.20, 5, +0.11	-0.26 ± 0.12, 4, +0.07	-0.76 ± 0.01, 2, -0.09	...	-0.4 ± 0.21, 3, +0.1
Mg II	7.58	-0.21 ± 0.18, 3, +0.10	-0.48 ± 0.10, 2, -0.15	-0.74, ±0.08, 2, -0.07	-2.8, 1, +0.2	-0.4, 1, +0.1
Si I	7.55	-0.37 ± 0.17, 3, -0.06	+0.08 ± 0.09, 9, +0.42	-0.20 ± 0.03, 2, +0.47
Si II	7.55	-0.39 ± 0.05, 2, -0.09	+0.23 ± 0.13, 2, +0.56	-0.10 ± 0.25, 2, +0.57	-2.4 ± 0.17, 2, +0.6	-0.1 ± 0.10, 7, +0.4
Si III	7.55	+0.0, 1, +0.5
S I	7.21	+0.04 ± 0.02, 2, +0.35	+0.08 ± 0.08, 3, +0.41	-0.30, 0.21, 2, +0.37
S II	7.21	-0.1 ± 0.20, 15, +0.6	+0.1 ± 0.18, 9, +0.6
Ca I	6.36	-0.18 ± 0.15, 9, +0.13	-0.18 ± 0.12, 22, +0.15	-0.59 ± 0.09, 7, +0.09
Ca II	6.36	-0.19, 1, +0.12	-0.26, 1, +0.07	-1.5 ± 0.05, 2, -1.0
Sc II	3.10	-0.07 ± 0.10, 10, +0.24	+0.01 ± 0.18, 11, +0.34	-0.39 ± 0.14, 7, +0.28	...	-0.6, 1, -0.1
Ti I	4.99	...	-0.25 ± 0.13, 4, +0.08
Ti II	4.99	-0.30 ± 0.15, 27, +0.01	-0.34 ± 0.16, 17, -0.01	-0.57 ± 0.19, 25, +0.10	...	-0.4 ± 0.15, 22, +0.1
V II	4.00	-0.03, 1, +0.28	-0.28 ± 0.28, 2, -0.05
Cr I	5.67	-0.27 ± 0.25, 4, +0.04	-0.23 ± 0.12, 10, +0.10	-0.59, 1, +0.09
Cr II	5.67	-0.24 ± 0.14, 19, +0.07	-0.25 ± 0.11, 14, +0.09	-0.44 ± 0.17, 23, +0.23	...	-0.5 ± 0.15, 13, -0.0
Mn I	5.39	-0.27, 1, +0.04	-0.31 ± 0.16, 5, -0.02	-0.49 ± 0.15, 3, +0.18
Mn II	5.39	-0.12 ± 0.27, 2, +0.11
Fe I	7.52	-0.30 ± 0.17, 87,.....	-0.28 ± 0.12, 136,	-0.71 ± 0.12, 33,
Fe II	7.52	-0.32 ± 0.13, 28,.....	-0.38 ± 0.12, 29,	-0.63 ± 0.11, 24,	< -3.0, <i>syn</i> ,	-0.5 ± 0.14, 36,
Co I	4.91	...	-0.42, 1, -0.09
Ni I	6.25	-0.17 ± 0.09, 6, +0.14	-0.24 ± 0.10, 17, +0.09
Ni II	6.25	-0.37 ± 0.22, 2, -0.06
Zn I	4.63	-0.36 ± 0.23, 2, -0.06
Sr II	2.90	-0.06, 1, +0.25	...	-1.03, 1, -0.36
Y II	2.24	-0.30 ± 0.07, 4, +0.01	-0.17 ± 0.21, 4, +0.16	-0.51 ± 0.18, 5, +0.16
Zr II	2.60	-0.34, 1, -0.03	-0.33 ± 0.01, 2, +0.00	-0.80, 1, -0.13
Ba II	2.13	-0.11 ± 0.13, 3, +0.20	+0.01 ± 0.05, 2, +0.34	-0.61 ± 0.12, 4, -0.06
Ce II	1.55	...	-0.12 ± 0.11, 2, -0.21
Eu II	0.51	...	-0.47, 1, -0.14

* Non-LTE corrected estimates.

surface of this object. This star resembles HD 107369 as described by Van Winckel (1997) in some respects. Its temperature and hydrogen lines profiles are similar, both objects are metal-poor with [Fe/H] of -1.0 and -0.7 for HD 107369 and HD 27381 respectively, and show a relative carbon deficiency and nitrogen enhancement. These two objects show in a milder form, the abundance pattern reported for hot post-AGB stars by Conlon et al. (1993).

3.4. HD 137569

The reddening-free indices $[m_1] = 0.062$, $[u - b] = 0.939$ and $[c_1] = 0.707$ when used with synthetic colors for model atmospheres of Kurucz (1993) led to a preliminary estimates of temperature and gravity. We have used Strömgen photometry

published in Mermillod (1998) and Newell & Graham (1976). The indices $[u - b]$ and $[c_1]$ are the measure of Balmer discontinuity, which for this temperature range is known to be a good temperature indicator, while it is not sensitive to gravity. This led us to a starting T_{eff} of 12000 K. A similar value is reported by Danziger & Jura (1970) These authors derive $\log g$ of 2.3 from the intersection of the H_{γ} profile and Balmer jump loci. More recently Behr (2003) estimated rotation velocity and atmospheric parameters by comparing the observed spectrum with the synthesized one. Behr estimated T_{eff} of 12073 ± 400 K, $\log g$ of 2.38 ± 0.4 , ξ of 0.0 ± 0.8 km s⁻¹ and $v \sin i$ of 18.5 km s⁻¹.

We had obtained one spectrum of the star in 2000 at the OHP and were intrigued by its appearance. Although the

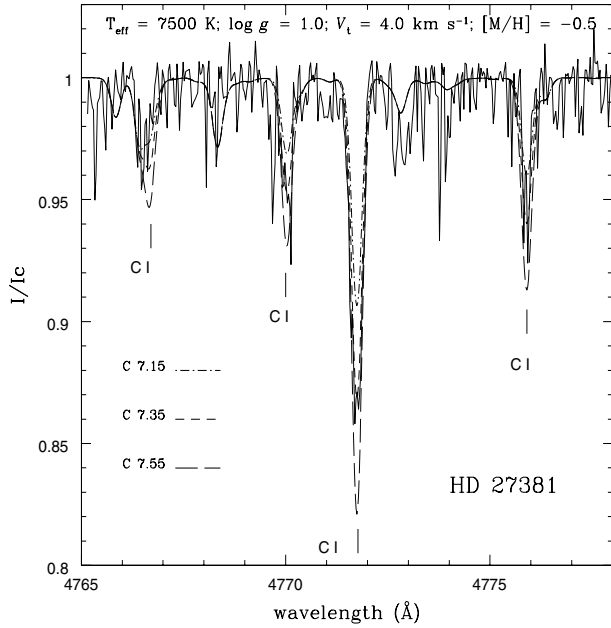


Fig. 2. Agreement between the synthesized and observed spectrum for carbon lines. The best fit is obtained for 7.35.

H I and He I lines were similar to that of a late B supergiant, the C II, Si II, Mg II and Fe II lines were extremely weak. Another spectrum using the 2.7 m telescope of McDonald Observatory was obtained with a resolution of 60 000 which enabled a spectral coverage of 3700 Å to 1 μ. A comparison of observed H_γ and H_δ profiles with those synthesized using $T_{\text{eff}} = 12\,000$ K and a range of gravities lead to $\log g = 2.0$. We have used the models by Jeffery et al. (2001) which extend to much lower gravities than those of Kurucz (1993). These models could also give a good match to the He I line at 4388 Å which is also gravity sensitive and to He I lines at 5015, 5047 Å which are very sensitive to temperature. We have shown in Fig. 3 the comparison between computed profiles for different gravities and the observed H_γ profile.

The estimated temperatures and gravities therefore have accuracies of ± 500 K and ± 0.5 dex. The N I lines have a wide range in equivalent width and therefore were used to derive ξ of 7 km s⁻¹. Our derived abundances for different elements are presented in Table 4. The agreement between the synthesized and observed spectrum for the spectral region covering the C, N, O region is presented in Fig. 4. The figure also contains the spectrum synthesized using the adopted atmospheric parameters and solar composition (shown as large dots in Fig. 4). It is obvious that the star is highly deficient in Fe. The lines of Fe II at 6147.7, 6149.3, 7462.4 are nearly absent in the observed spectrum.

At the temperature of 12 000 K, non-LTE effects are expected to be large. Przybilla et al. (2001, 2000) have carried out a very extensive non-LTE analysis of C, N, O elements for stars in the 9000 to 12 500 K temperature range. The star β Ori studied by them has atmospheric parameters ($T_{\text{eff}} = 12\,500$ K, $\log g = 1.8$) very similar to those of HD 137569 and the investigation employs the same lines. Therefore the non-LTE correction calculated for β Ori may be used for HD 137569. After

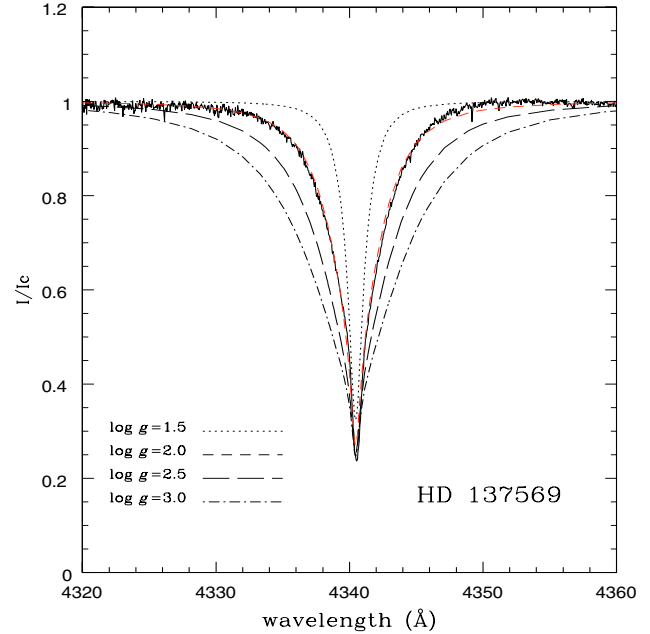


Fig. 3. H_γ profile of HD 137569. The models correspond to T_{eff} 12 000 K and gravities 1.5, 2.0, 2.5 and 3.0. The best fit is obtained for $\log g = 2.0$.

applying a non-LTE correction of -0.4 for C II, -0.6 for N I and -0.30 for O I lines we present the non-LTE corrected estimates in bold in Table 4.

The derived deficiency of C accompanied by N enhancement indicates that the CN processed material is brought to the surface via dredge-up. The carbon deficiency found for HD 137569 is not as large as in other hot post-AGB stars. A more remarkable feature is the total absence of Fe II lines. We could only get an upper estimate of -3.0 for [Fe/H]. The weak Si II and Mg II lines also led to [Si/H] and [Mg/H] of -2.4 and -2.8 respectively. On the other hand the S II and Ne I lines indicate near solar abundance. These abundances are derived using a sufficiently large number of lines and hence are quite robust. The selective depletion of easily condensable elements with higher condensation temperatures has been observed in a large number of post-AGB stars. Well known examples are HR 4049 (Lambert et al. 1988) and HD 44179 (Van Winckel 1995). A similar phenomenon has also been found in many RV Tau stars (Giridhar et al. 2005; Maas 2002, and references therein). The elements S and Zn have a lower condensation temperature and are generally unaffected by this effect. In fact these elements are considered better metallicity indicators. However, S and Zn abundances are not available for many hot post-AGB stars.

Although this phenomenon is well studied in post-AGB stars of intermediate temperatures, its presence in hot post-AGB stars is not yet established. We are only aware of LS IV -4°01 and LB 3193 showing incomplete suggestions of selective depletion of refractory elements. We have compared the abundances of HD 137569 with other hot post-AGB candidates and two PNe given in Table 5. We have plotted in Fig. 5 the observed abundances of the stars included in Table 5 as a function of the most recent condensation temperatures

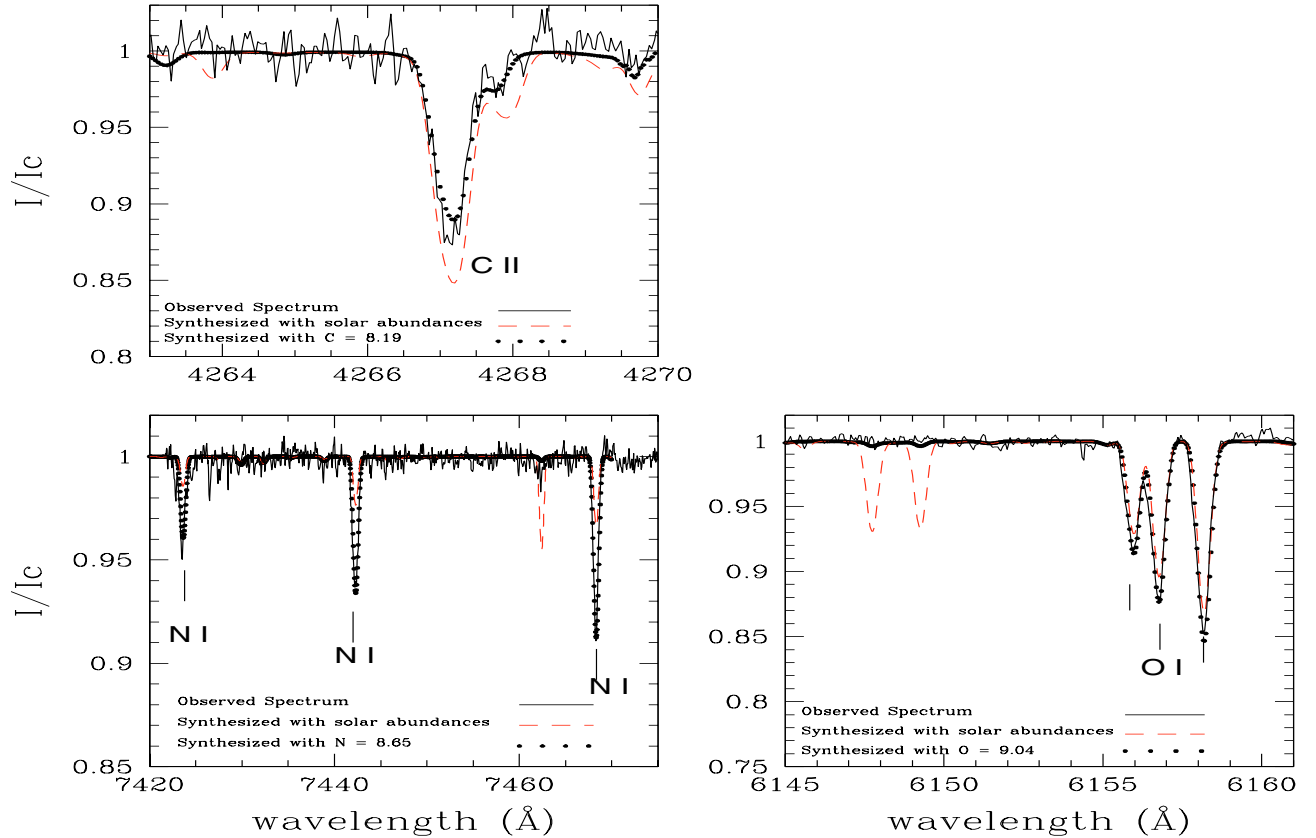


Fig. 4. The agreement between the synthesized and observed spectrum for spectral regions containing C, N and O lines for HD 137569.

Table 5. Abundances for HD 137569 compared with other post-AGB and PNe stars.

Star	T_{eff}	[C/H]	[N/H]	[O/H]	[Mg/H]	[Si/H]	[S/H]	[Fe/H]
LS IV $-4^{\circ}01^1$	11 000	<-1.21			-1.98	-2.05		
LS IV $-4^{\circ}01^8$	10 000				-2.78	-1.68		-1.71
HD 137569²	12 000	-0.60	+0.20	+0.05	-2.80	-2.40	-0.10	<-3.0
LB 3193 ¹	12 900	<-1.91			-2.08	-2.15		
PG 1323-086 ³	16 000	<-2.25	-0.98	-0.77	-1.71	-1.37		
PG 1704+222 ³	18 000	-1.40	-0.89	-0.85	-1.37	-1.13		
PHL 174 ⁴	18 200	<-2.31	-1.11	-0.85	-1.38	-1.05		
Barnard 29 ⁵	20 000	-2.16 ⁴	-0.61	-1.15 ¹		-1.25 ⁵		-2.2 ⁵
BD +33 ⁰ 2642 ⁶	20 200	-0.93	-0.56	-0.62	-1.1	-0.9		
LB 3219 ¹	21 400	-1.71	-0.31	-1.15	-0.58	-0.95		
ROA 5701 ⁵	24 000	-2.57	-1.04	-0.78		-1.41		-2.71
LS IV $-12^{\circ}111^1$	24 000	-1.71	-0.11	+0.05	-0.28	+0.05	-0.6	-0.41
LS IV $-12^{\circ}111^7$	24 000	-0.63	+0.29	+0.05	-0.28	+0.08	-0.5	

References: (1) McCausland et al. (1992), (2) this work, (3) Moehler & Heber (1998), (4) Conlon et al. (1991), (5) Moehler et al. (1998), (6) Napiwotzki et al. (1994), (7) Conlon et al. (1993), (8) Mooney et al. (2002).

presented by Lodders (2003). It might have been more instructive to plot the abundances of these elements relative to S or Zn but these abundances are not available for many post-AGB stars. The depletion of refractory elements is an attractive but yet to be substantiated possibility for stars cooler than 13 000 K. Efforts are required to measure sulphur abundances

in hot post-AGB candidates. The large depletion only of refractory elements gives strong support to the post-AGB candidature of HD 137569. The explanation of these abundance peculiarities found in post-AGB stars requires a site of dust-gas separation. The suggestion of dust-gas separation occurring in a circumbinary disk is gaining more support with the

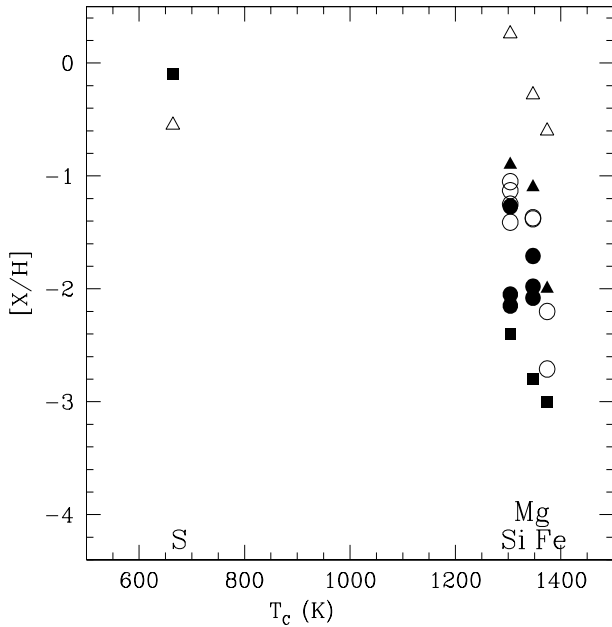


Fig. 5. Elemental abundance plotted as a function of condensation temperature. Filled symbols represent relatively cool stars and open symbols represent hotter stars. Triangles represent PNe stars following the same convention. The post-AGB stars are shown as circles. Filled squares are the values for HD 137569 for which the depletion due to condensation is quite evident.

increase in detected binaries among post-AGB stars. HD 137569 is known to be a single lined spectroscopic binary with a period of 529.8 days and a systemic velocity of -45 km s^{-1} as reported by Bolton & Thomson (1980). This might strengthen our suggestion that HD 137569 is a post-AGB star. Lack of IRAS fluxes might be caused by a longer transition time. The derived temperature and gravity places the star very near the post evolutionary track of Schönberner (1983) for a mass of $0.546 M_{\odot}$. The C, N, O abundances of HD 137569 resemble with those for PN LS IV $-12^{\circ}111$ (Conlon et al. 1993).

The UV spectra of this object would be extremely useful for the better coverage of Fe-group elements.

3.5. HD 172324

HD 172324 is a hot star at high galactic latitude, showing emission components in the hydrogen line profiles. It is a high radial velocity star and velocities around -110 km s^{-1} are seen. We observed the stars in 1995, 1999, 2000 and 2003 and found radial velocity variations larger than the measurement errors. The measured heliocentric radial velocities are given in Table 2. The star is listed as a possible variable star in the catalog of Rufener (1981).

We have obtained high resolution spectra of this object at different epochs and found very interesting variations in H_{α} and H_{β} as displayed in Fig. 6. The H_{α} profile is seen mostly in emission. H_{β} has a sharp central emission, rising above the continuum level on March 2003, and a broad absorption line. The spectrum contains a large number of He I lines. We have used the excitation and ionization equilibrium of Fe, Mg and

Si to derive $T_{\text{eff}} = 10\,500 \text{ K}$, $\log g = 2.5$ and $\xi = 7.0 \text{ km s}^{-1}$. The presence of a strong O I triplet at 7774 \AA also supports the derived low gravity for this star. The lines used for CNO abundances are the same as those used for HD 137569. We have derived almost solar values $[\text{C}/\text{H}] = -0.04$, $[\text{N}/\text{H}] = +0.71$ and $[\text{O}/\text{H}] = +0.25$ for this star. At the temperature of $10\,500 \text{ K}$, departure from non-LTE conditions are likely to be significant. Using the non-LTE correction for C II feature tabulated by Przybilla et al. (2001) for stars in the temperature range 9000 to $12\,500 \text{ K}$, we have estimated a non-LTE correction of -0.3 hence the corrected $[\text{C}/\text{H}] = -0.34$. Similarly, using non-LTE corrections of -0.6 for N I (Przybilla & Butler 2001) that of -0.3 for O I (Przybilla et al. 2000) we have derived the corrected values of $[\text{N}/\text{H}] = +0.11$ and $[\text{O}/\text{H}] = -0.05$, i.e. nearly solar values for HD 172324. These abundances are very similar to the CNO estimates derived for a sample of population I B type supergiants (Gies & Lambert 1992). However, consistently large radial velocity derived at 4 epochs and $[\text{Fe}/\text{H}] = -0.5$ makes it a very intriguing object.

We were surprised by the absence of the Na I 8195 \AA feature in our spectrum. For $\eta \text{ Leo}$ ($T_{\text{eff}} \sim 10\,200 \text{ K}$), Takeda & Takada-Hidai (1994) have reported a strength of 30 m\AA . Since the temperature of HD 172324 is very similar, the non-detection of the above Na feature would imply that $[\text{Na}/\text{H}] \leq -0.8$. For a sample of A-F supergiants, these authors have reported an overabundance of Na possibly caused by the mixing of NeNa-cycle products from the hydrogen burning zone. Absence of Na overabundance indicates that the NeNa-cycle products have not been brought to the surface. On the other hand, Ne I lines are very strong, indicating $[\text{Ne}/\text{H}] = +0.4$.

It appears that similar to A supergiants studied by Venn (1995b) the evolution of HD 172324 avoided extensive mixing at the red giant phase by evolving directly from the main sequence to their present position. Relative to iron, Ne, Si, and S show the mild enrichment normally seen in metal-poor objects.

The radial velocity of this star shows significant variation as can be seen in Table 2. The same is true for hydrogen line profiles where the strength of emission components show large variations. Our high resolution spectrum of this star shows distinct doubling for O I lines in the 7774 \AA triplet components. We therefore believe it may be a pulsating variable or a binary star.

3.6. Cool stars

These stars were included in our sample due to IR flux detection and their high galactic latitudes. We could measure a very large number of lines for each element and for many elements lines of two stages of ionization could be used. We used the excitation and ionization equilibrium of Fe, Cr and Ti to derive T_{eff} , $\log g$ and ξ .

HD 10132 has a significantly large radial velocity of -70 km s^{-1} . Carbon is deficient, possibly caused by CN processing. Among α elements, sulfur shows a mild enrichment relative to iron. Fe-peak elements and (within the measurement errors) s-process elements show near solar abundances. Similarly, HD 159251 shows near solar abundance for most of

Table 6. Abundances of cooler stars.

Species	log ϵ_{\odot}	HD 10132	HD 12533	HD 159251
		[X/H], <i>n</i> , [X/Fe]	[X/H], <i>n</i> , [X/Fe]	[X/H], <i>n</i> , [X/Fe]
C I	8.39	$-0.43 \pm 0.11, 2, -0.39$
O I	8.69	$-0.20, 1, -0.16$
Na I	6.33	$-0.04 \pm 0.19, 4, +0.01$	$+0.14 \pm 0.16, 2, +0.20$	$-0.10 \pm 0.03, 2, -0.06$
Mg I	7.58	$-0.18 \pm 0.37, 3, -0.14$	$-0.24, 1, -0.18$	$-0.67, 1, -0.63$
Al I	6.47	$-0.35 \pm 0.14, 3, -0.31$	$-0.15, 1, -0.09$	$-0.21 \pm 0.09, 2, -0.17$
Si I	7.55	$+0.03 \pm 0.16, 16, +0.08$	$+0.14 \pm 0.25, 8, +0.20$	$+0.04 \pm 0.11, 20, +0.09$
S I	7.21	$+0.15 \pm 0.11, 2, +0.20$
K I	5.12	...	$+0.21, 1, +0.27$...
Ca I	6.36	$+0.05 \pm 0.20, 11, +0.10$	$-0.20 \pm 0.19, 10, -0.14$	$-0.21 \pm 0.25, 25, -0.17$
Sc I	3.10	...	$-0.12 \pm 0.16, 7, -0.06$	$-0.16 \pm 0.15, 10, -0.11$
Sc II	3.10	$+0.36 \pm 0.17, 9, +0.41$	$-0.03 \pm 0.20, 5, +0.03$	$+0.10 \pm 0.32, 9, +0.15$
Ti I	4.99	$-0.07 \pm 0.16, 20, -0.03$	$-0.19 \pm 0.17, 38, -0.13$	$-0.13 \pm 0.21, 81, -0.09$
Ti II	4.99	$+0.04 \pm 0.10, 5, +0.09$	$-0.22 \pm 0.25, 4, -0.16$	$-0.07 \pm 0.09, 5, -0.03$
V I	4.00	$-0.05 \pm 0.24, 15, -0.01$	$+0.01 \pm 0.24, 31, +0.07$	$0.03 \pm 0.20, 35, +0.08$
V II	4.00	$+0.17, 1, +0.22$
Cr I	5.67	$-0.03 \pm 0.19, 19, +0.02$	$-0.16 \pm 0.20, 22, -0.10$	$-0.07 \pm 0.22, 35, -0.03$
Cr II	5.67	$-0.09 \pm 0.20, 10, -0.05$	$+0.04 \pm 0.25, 2, +0.10$	$+0.07 \pm 0.16, 7, +0.12$
Mn I	5.39	$+0.20 \pm 0.20, 5, +0.25$	$+0.01 \pm 0.21, 6, +0.07$	$+0.02 \pm 0.31, 16, +0.07$
Fe I	7.52	$-0.01 \pm 0.14, 94, \dots$	$-0.08 \pm 0.18, 132, \dots$	$-0.03 \pm 0.16, 253, \dots$
Fe II	7.52	$-0.08 \pm 0.12, 19, \dots$	$-0.04 \pm 0.22, 11, \dots$	$-0.06 \pm 0.12, 18, \dots$
Co I	4.92	$-0.07 \pm 0.18, 6, -0.03$	$-0.02 \pm 0.25, 11, +0.04$	$+0.17 \pm 0.24, 23, +0.22$
Ni I	6.25	$-0.07 \pm 0.17, 27, -0.03$	$-0.05 \pm 0.17, 38, +0.01$	$-0.04 \pm 0.24, 88, +0.01$
Cu I	4.26	$+0.41 \pm 0.33, 3, +0.46$
Zn I	4.60	$-0.14 \pm 0.04, 2, -0.10$	$-0.05, 1, +0.01$	$-0.14 \pm 0.20, 2, -0.09$
Sr I	2.90	$-0.21, 1, -0.16$
Y I	2.24	...	$-0.24 \pm 0.16, 2, -0.18$...
Y II	2.24	$-0.05 \pm 0.13, 4, +0.00$	$-0.12 \pm 0.15, 3, -0.06$	$-0.06 \pm 0.21, 3, -0.01$
Zr I	2.60	$-0.10 \pm 0.12, 6, -0.05$
Zr II	2.60	$+0.12 \pm 0.04, 2, +0.17$	$-0.26 \pm 0.16, 9, -0.20$	$+0.29, 1, +0.34$
Mo II	1.92	...	$+0.04 \pm 0.10, 2, +0.10$	$-0.01, 1, +0.04$
Ba II	2.13	$+0.19 \pm 0.09, 2, +0.24$	$+0.23, 1, +0.29$	$+0.02 \pm 0.13, 2, +0.07$
La II	1.22	$-0.17 \pm 0.04, 3, -0.13$	$+0.13 \pm 0.18, 2, +0.19$	$-0.18 \pm 0.14, 3, -0.13$
Ce II	1.55	$+0.02 \pm 0.20, 3, +0.07$	$-0.01 \pm 0.15, 4, +0.05$	$-0.09 \pm 0.21, 4, -0.04$
Pr II	0.71	...	$+0.34, 1, +0.40$	$+0.16 \pm 0.10, 2, +0.21$
Nd II	1.50	$-0.11 \pm 0.17, 6, -0.07$	$0.12 \pm 0.54, 5, -0.06$	$-0.16 \pm 0.18, 5, -0.11$
Sm II	1.00	$+0.01 \pm 0.30, 2, +0.06$
Eu II	0.51	$-0.04 \pm 0.07, 2, +0.01$...	$+0.17, 1, +0.22$

the elements. However, these abundances are the only spectroscopic estimates made based on a very large number of lines. These estimates could be used for the calibration of photometric indices of cool stars.

Because of its binarity, HD 12533 was included in the barium star survey of Začs (1994), but it was not found to show significant enhancement of Ba and other s-process elements. Our present analysis uses better resolution spectra and much

larger spectral coverage, and therefore includes much larger number of lines for each species. In spite of the low temperature, the spectrum is not overcrowded. We confirm a lack of enhancement for Ba and other s-process elements reported by Začs and find near solar abundances for the other elements. We do not confirm the $[\text{Fe}/\text{H}] = -0.4$ estimated by Začs. Our derived temperature (4250 K) is slightly smaller than that derived by Začs (4350 K) and we derive higher gravity ($\log g = 2.0$)

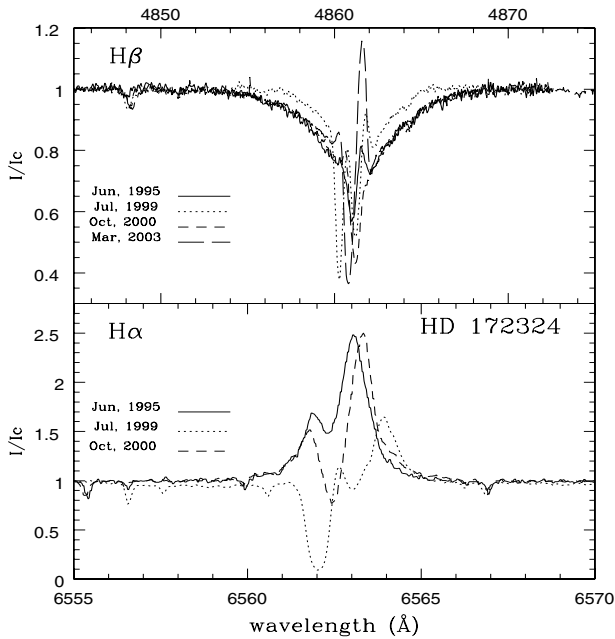


Fig. 6. $H\alpha$ and $H\beta$ variations in HD 172324.

than that of Začs ($\log g = 0.5$). In the light of the better quality of data used and the extensive spectral coverage, the abundances presented in Table 4 are likely more accurate.

4. Conclusions

The present work is a continuation of Paper I extending to high temperature regimes of the post-AGB candidates. HD 27381 appears to be very similar to the post-AGB star HD 107369. These two stars are candidates for a search for light variability and better spectral coverage as they appear intermediate between cooler post-AGB stars with exotic abundances and hot post-AGB stars.

Another important finding of the present work is the abundance peculiarities exhibited by HD 137569. It shows selective depletion of the refractory elements as seen in the case of HR 4049 and other well-known post-AGB stars and many RV Tau stars. It is relatively cooler than the hot post-AGB stars studied by Conlon et al. (1991) and McCausland et al. (1992) but two objects, LS IV-4°01 and LB 3193 which are of similar temperature, show a similar deficiency of Mg and Si. A large number of post-AGB stars showing depletion of refractory elements are found to be binaries. HD 137569 is known to be a spectroscopic binary but the lack of IR fluxes of this object might be due to mass ejection having occurred long ago. The carbon deficiency observed for this star is not as large as that seen for the hot post-AGB stars. On the other hand the derived CNO abundances are similar to PNe abundances. HD 172324 is a moderately metal-poor, high velocity star that does not resemble post-AGB stars in abundance pattern, but deserves continuous photometric and radial velocity monitoring in search of binarity and/or pulsation. HD 10285 and HD 25291 do not appear to be post-AGB stars but show evidence of red giant mixing that has brought the products of

the NeNa cycle to the surface. The rest of the stars appear to be normal stars of near solar composition.

Investigation of high galactic latitude supergiants with light variability could be quite rewarding even if the criteria of two peaks in the SED is not met. These might be post-AGB stars with progenitors of lower masses. Here the transition time being larger, these stars might have lost most of their envelope before moving towards the high temperature regime and may be left with sparse and cold circumstellar matter (if present). To the best of our knowledge BD+39°4926 is the only outlier object among post-AGB stars, showing depletion of refractory elements but without IR excess. HD 137569 appears to be a new addition to the family.

Acknowledgements. We express our gratitude to the anonymous referee for many important suggestions. We are indebted to Drs. E. Reddy and D. Young for obtaining some spectra for us. We thank Dr. Gajendra Pandey for his help with high temperature low gravity model atmospheres. We also acknowledge the support from DGAPA-UNAM grant through project IN110102 and are thankful to the CONACyT (Mexico) and the Department of Science and Technology (India), for the travel support and local hospitality respectively under Indo-Mexican collaborative project DST/INT/MEXICO/RP001/2001. This work has made use of the SIMBAD database.

References

- Allende Prieto, C., Lambert, D. L., & Asplund, M. 2001, *ApJ*, 556, 63
- Allende Prieto, C., Lambert, D. L., & Asplund, M. 2002, *ApJ*, 573, 137
- Andrievsky, S. M., Egorova, I. A., Koroti, S. A., & Burnage, R. 2002, *A&A*, 39, 519
- Arellano Ferro, A., Giridhar, S., & Mathias, P. 2001, *A&A*, 368, 250 (Paper I)
- Baranne, A., Queloz, D., Mayor, M., et al. 1996, *A&AS*, 119, 373
- Behr, B. B. 2003, *ApJS*, 149, 101
- Bidelman, W. P. 1990, in *Luminous High-Latitude Stars*, ASP Conf. Ser., 45, 47
- Bolton, C. T., & Thomson, J. R. 1980, 241, 1045
- Bravo-Alfaro, H., Arellano Ferro, A., & Schuster, W. H. 1997, *PASP*, 109, 958
- Conlon, E. S., Dufton, P. L., Keenan, F. P., & McCausland, R. J. H. 1991, *MNRAS*, 248, 820
- Conlon, E. S., Dufton, P. L., McCausland, R. J. H., & Keenan, F. P. 1993, *ApJ*, 408, 593
- Danziger, I. J., & Jura, M. A. 1970, *ApJ*, 161, 997
- Gies, D. R., & Lambert, D. L. 1992, *ApJ*, 387, 673
- Gilmore, G., Wyse, R. F. G., & Jones, J. B. 1995, *AJ*, 109, 1095
- Giridhar, S., & Arellano Ferro, A. 1995, *Rev. Mex. Astron. Astrofis.*, 31, 23
- Giridhar, S., Lambert, D. L., & Gonzalez, G. 1998, *ApJ*, 509, 366
- Giridhar, S., Lambert, D. L., & Gonzalez, G. 2000, *ApJ*, 531, 521
- Giridhar, S., Lambert, D. L., Reddy, B. E., Gonzalez, G., & Yong, D. 2005, *ApJ*, 627, 432
- Gray, R. O., & Corbally, C. J. 1994, *AJ*, 107, 742
- Grevesse, N., Noels, A., & Sauval, A. J. 1996, *ASP Conf. Ser.*, 99, 117
- Jeffery, C. S., Woolf, V. M., & Pollaco, D. L. 2001, *A&A*, 376, 497
- Kupka, F., Piskunov, N., Ryabchikova, T. A., Stempels, H. C., & Weiss, W. W. 1999, *A&AS*, 138, 119
- Kurucz, R. L. 1993, *ATLAS9 Stellar atmosphere Programs and 2 km s⁻¹ grid CDRoM Vol. 13* (Cambridge: Smithsonian Astrophysical Observatory)

- Lambert, D. L., Hinkle, K. H., & Luck, R. E. 1988, *ApJ*, 333, 917
Lambert, D. L., Heath, J. E., Lemke, M., & Drake, J. 1996, *ApJS*, 103, 183
Lodders, K. 2003, *ApJ*, 591, 1220
Luck, R. E. 2002, private communication
Maas, T., Van Winckel, H., & Waelkens, C. 2002, *A&A*, 386, 504
McCausland, R. J. H., Conlon, E. S., Dufton, P. L., & Keenan, F. P. 1992, *ApJ*, 394, 298
Mermilliod, H. B. 1998, *A&AS*, 129, 431
Moehler, S., & Heber, U. 1998, *A&A*, 335, 985
Moehler, S., Heber, U., Lemke, M., & Napiwotzki, R. 1998, *A&A*, 339, 537
Mooney, C. J., Rolleston, W. R. J., Keenan, F. P., et al. 2002, *MNRAS*, 337, 851
Napiwotzki, R., Heber, U., & Koeppen, J. 1994, *A&A*, 292, 239
Newell, B., & Graham, J. A. 1976, *ApJ*, 204, 804
Prochaska, J. X., Naumov, S. O., Carney, B. W., McWilliam, A., & Wolfe, A. M. 2000, *AJ*, 120, 2513
Przybilla, N., & Butler, K. 2001, *A&A*, 379, 955
Przybilla, N., Butler, K., Becker, S. R., Kudritzki, R. P., & Venn, K. A. 2000, *A&A*, 359, 1085
Przybilla, N., Butler, K., & Kudritzki, R. P. 2001, *A&A*, 379, 936
Qiu, H., Zhao, G., Chen, Y., & Li, Z. 1999a, *Publ. Beijing Astron. Obs.*, 33, 34
Qiu, H., Zhao, G., & Li, Z. 1999b, *Publ. Beijing Astron. Obs.*, 33, 58
Reddy, B. E., Lambert, D. L., Gonzalez, G., & Yong, D. 2002, *ApJ*, 564, 482
Rufener, F. 1981, *A&AS*, 45, 207
Schönberner, D. 1983, *ApJ*, 272, 708
Snedden, C. 1973, Ph.D. Thesis, Univ. of Texas at Austin
Takeda, Y., & Takada-Hidai, M. 1994, *PASJ*, 46, 395
Trams, N. R., Waters, L. B. F. M., Lamers, H. J. G. L. M. R., et al. 1991, *A&AS*, 87, 3
Tull, R. G., Macqueen, P. J., Sneden, C., & Lambert, D. L. 1995, *PASP*, 107, 251
van der Veen, W. E. C. J., & Habing, H. J. 1988, *A&A*, 194, 125
Van Winckel, H. 1995, *A&A*, 293, L25
Van Winckel, H. 1997, *A&A*, 319, 561
Van Winckel, H. 2003, *ARA&A*, 41, 391
Venn, K. A. 1995a, *ApJS*, 99, 659
Venn, K. A. 1995b, *ApJ*, 449, 832
Wiese, W. L., Führ, J. R., & Deters, T. M. 1996, *J. Phys. Chem. Ref. data Monograph No. 7*
Začs, L. 1994, *A&A*, 238, 937